XL CILAMCE
IBERO-LATIN AMERICAN CONGRESS ON COMPUTATIONAL METHODS IN ENGINEERING
NOVEMBER 11-14, 2019
Praiamar Natal Hotel & Convention
Natal, RN-BRAZIL

THREE-DIMENSIONAL NUMERICAL SIMULATION OF A CENTRIFUGAL COMPRESSOR OPERATING WITH SUPERCRITICAL CO2

Allan Moreira de Carvalho
Bruno José Nagy Antonio
allan.carvalho@aluno.ufabc.edu.br
bruno.nagy@ufabc.edu.br
Federal University of ABC
Av. dos Estados, 5001 - Bangú, 09210-580, Santo André/SP, Brazil
Fábio Saltara
Jurandir Itizo Yanagihara
fsaltara@usp.br
jiy@usp.br
University of São Paulo
Av. Prof. Luciano Gualberto, 380 - travessa do politécnico, 05508-010, São Paulo/SP, Brazil
Paulo Eduardo Batista de Mello
pmello@fei.edu.br
University Center FEI
Av. Humberto de Alencar Castelo Branco, 3972-B - Assunção, 09850-901, São Bernardo do Campo/SP, Brazil
Leandro Oliveria Salviano
University of São Paulo State
leandro.salviano@unesp.br
Av. Brasil Sul, 56 - Centro, 15385-000. Ilha Solteira/SP, Brazil
Daniel Jonas Dezan
daniel.dezan@ufabc.edu.br
Federal University of ABC
Av. dos Estados, 5001 - Bangú, 09210-580, Santo André/SP, Brazil

Abstract. Centrifugal compressors performance can be benefited by the low viscosity, high density and small compression work of the supercritical CO2. The design and aerodynamic optimization of such devices must take into account the flow behaviour under these conditions, that can be ensured by high fidelity three-dimensional computational fluid dynamic simulations. This work presents a numerical modeling and simulation of the highly turbulent, compressible flow inside the impeller of the proof-of-concept supercritical CO2 microcompressor experimentally tested at Sandia National Laboratories. The steady state solution was obtained by solving the three-dimensional Reynolds Averaged Navier-Stokes equations using the comercial software ANSYS CFX. The equation system was closed by the Shear Stress Transport turbulence model. Thermodynamic properties were evaluated through the Aungier version of Redlich-Kwong equation of state, providing better accuracy near critical point condition than its original version. A grid convergence study was conducted to verify possible numerical error induced by computational domain discretization. Finally the numerical method was validated against experimental data and the flow characteristics, typical to centrigual compressors, like the suplementary depression and leakage flow losses was discussed.

Keywords: Centrifugal Compressor, Supercritical C02, Computational Fluidynamics

1 Introduction

While turbomachinery technology for steam and air as working fluids are very consolidated, investigations on power cycles operating with supercritical CO_2 started being exploited in 1960s, by **(author?)** [Angelino] and **(author?)** [Feher]. Since then, it became clear that many other applications could be benefited from small work needed to compress supercritical CO_2 due to its high density and low viscosity. These applications includes solar power plants **(author?)** [Zhang et al.], Brayton power cycles **(author?)** [Wright et al.], and because of the high pressure ratios achievable by centrifugal compressors, Carbon Capture and Storage (CCS). The last one comprises one of the bests present efforts to reduce the atmospherical CO_2 emissions, until 2015 CCS was estimated to represent 19% of the total CO_2 emissions worldwide supressed, **(author?)** [Fu and Gundersen].

The successful implementation of CCS on large scale will mostly depends onrobust and a high efficient technologies operating with supercritical CO_2. As the centrifugal compressor represents the main compression and pumping machine used on CCS, any mitigation of its aerodynamic losses comprises a very relevant challenge to all designer focused on the development of future CCS technologies.

Since the advent of the centrifugal compressors up to now, the design process of such turbomachines relies on one-dimensional analysis of the internal flow, frequently called mean line analysis. Despite of its simple mathematical formulation, this method can lead to very accurate results if empirical losses models are properly aplied. As a counterpart, the calibration of the losses models requires a lot of experimentation work rising up the development costs. Computing power experimented fast increase on the last decades allowing designers to replace the ancient experimental methods by modern numerical simulations of complex three-dimensional flow present on centrifugal compressors. This created another problem, the settlement of numerical models capable to predict the behaviour of the rotating viscous flow of supercritical fluids.

Multiphase flow and supercritical fluidynamics represents a very big challenge to be overcome. Not only the flow field on a centrifugal compressor is very complex by its rotating nature, but also the low flow coefficient involved represents a source for increased aerodynamic losses associated with friction, end-wall and parasitic losses, **(author?)** [Baltadjiev et al.] and **(author?)** [Lettieri et al.]. There are also several sources of difficulties when simulating this fluid flow: the absence of models for turbulent heat flux near critical point, **(author?)** [Pecnik et al.], the onset of unsteady phenomena near surge and choke conditions, **(author?)** [Abramian and Howard, Lennemann and Howard, Guo et al.] and the choice of a turbulence model fitted to hihgly turbulent flow, with boundary layer separation, reattachment, strong surface curvature and rotation influences, **(author?)** [Johnston].

This work presents methodologies to perform the computational fluidynamics simulation of a centrifugal compressor operating near the supercritial condition of CO_2. The proof-of-concept supercritical CO_2 microcompressor developed at Sandia National Laboratories **(author?)** [Wright et al.] was selected to be the validation model. A grid convergence study was conducted in order to investigate numerical errors related to domaind discretization, three degrees of refinment was performed. The numerical results was then validated against experimental dada, showing the numerical model resulted in a very accurate simulation. Finally, the results was presented with a brief discussion of the thermodynamics and fluid structure phenomena expected to occur on the impeller fo a centrifugal compressor.

2 Fluid Dynamics Modeling

The flow field inside the impeller is completelly described by the mass, momentum and energy conservation equations. This set of equations was solved by a finite volume method, using a turbomachinery specialized computation fluid dynamics software. Direct solving the governing equations is not an options as it would take a very long computing time. Solving the equations on a reasonable time without losing important physical phenomena require some assumptions to be made, in this work the fluid flow is considered to be:

- Compressible

- Viscous
- Turbulent
- At steady state condition

In order to capture unsteady turbulent phenomena the governing equations was solved on its Reynolds Avareged Navier Stokes formulation with a system closure made by the state-of-art $k - \omega$ SST (Shear Stress Transport) turbulence model.

2.1 Supercritial Thermodynamics

On the viscinity of critical point, supercritical fluids are expected to experience abrupt variations of its thermodynamic properties, so the ideal gas relations are no longer valid. An accurate prediction of the thermodynamic properties without compromising performance was carried by using the Aungier revisited version of Redlich-Kwong equation of state, **(author?)** [Aungier]. This equation of state was adjusted to reduce the deviation with respect to real gas properties near the critical point.

Figure 1 shows the variation of the specific heat at constant pressure and the ratio of specific heats for commom used equations of state, Redlich-Kwong , Peng Robinson and Span and Wagner. The issues near critical point is an unavoidable source of numerical error.

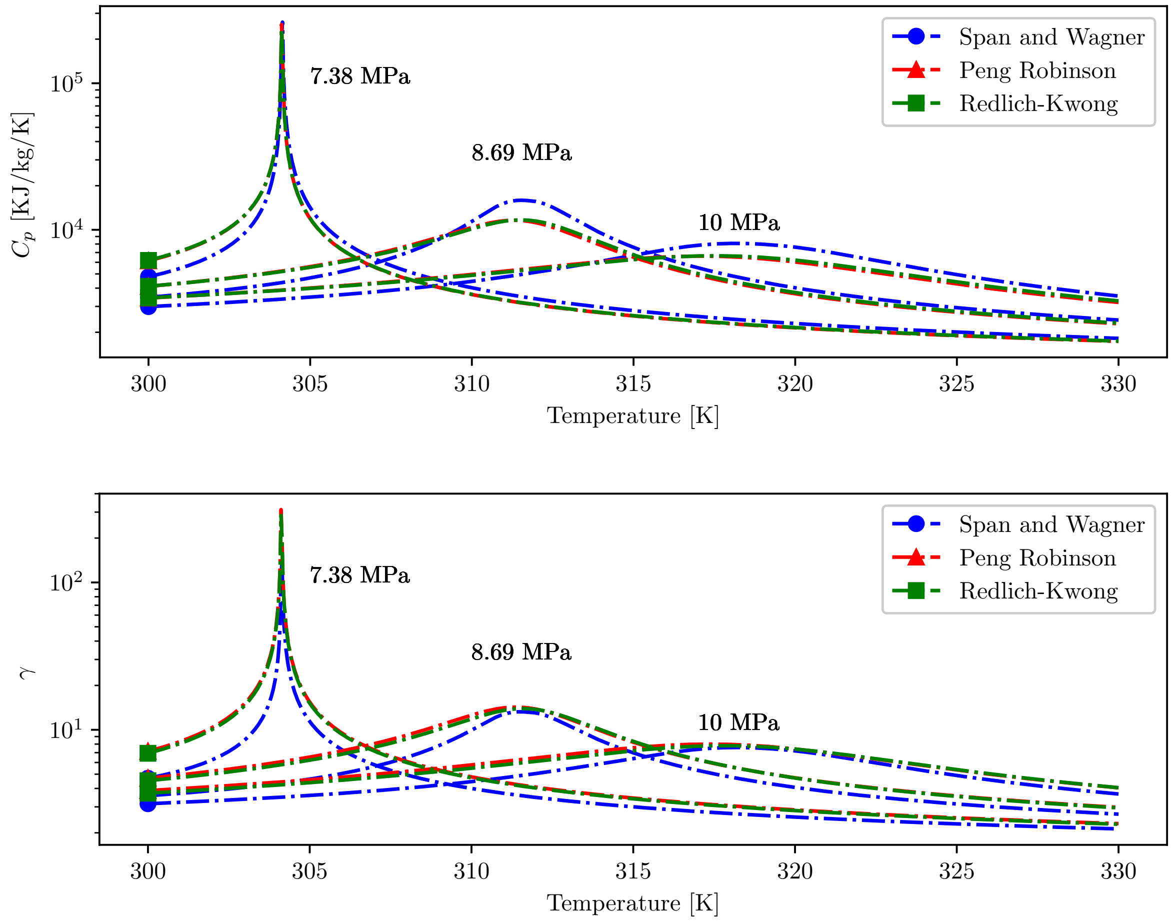

Figure 1. Common used equations of state evaluated near CO_2 critical point.

3 The SANDIA supercritical CO_2 microcompressor

Due to the supercritial CO_2 potential for high efficiency on power cycles, given its low critical temperature, Sandia National Laboratories conducted a recent research on advanced Brayton cycles using it as a working fluid. As a result, a proof-of-concept supercritical CO_2 microcompressor was designed and manufactured to investigate the issues related to the supercritical CO_2 compression, **(author?)** [Wright et al.].

In fact, the design point operation was not sustainable, but there was a lot of experimental data at off-design conditions over a $45000 \sim 55000$ RPM range. The stable operation at 55000 RPM was selected for our steady-state computational fluidynamics simulations presented at Table 1.

Table 1. Operational and design point of Sandia sCO_2 microcompressor.

Property	*Design Point*	*Operational Point*
T_{01}	305.3 K	306.4 K
P_{01}	7.69 MPa	7.89 MPa
$\dot{m}$	3.53 kg/s	2.043 kg/s
RPM	75000	55000
PR	1.81	1.27

3.1 Geometrical description

The complete three-dimensional geometry of the impeller involves complex mathematical description of the surfaces, for this purpose the software ANSYS TurboGrid was employed. The blade angle distributions, hub and shroud countours can be defined based on basic one-dimensional parameters, all the essencial data needed are summarized on Table 2.

The unshrouded impeller consists of six main blades and six additional splitter blades that have a lenght ratio of 0.7. Either main or splitter blades have a constant thickness distribution.

As long as supercritical CO_2 compressors is an strategic technology, not all geometrical parameters could be found on the official SANDIA National Laboratiories report. In those cases, these paremeters was estimated based on others attempts to perform numerical simulations of that impeller, **(author?)** [Meroni et al., Monge, Pecnik et al., Rinaldi et al.] and **(author?)** [Rinaldi et al.]. Because there was no information about wrap angle, that parameter was adjusted to comply with the main blade lenght.

4 Numerical Setup

The ANSYS CFX solver uses a finite-volume method to solve the discretized mass, momentum and energy equations. A full implicit, second-order interpolated Rhie and Chow method was selected to solve the system of momentum and mass conservation equations simultaneously, avoinding the expensive interactive process of SIMPLE algorithms. The advection terms was discretized by a high resolution scheme. The local time scale was set to conservative and only a relaxation over energy equation was employed to prevent unrealistic temperature predictions.

4.1 Computational Domain

This work uses a structurated hexahedral mesh. This type of mesh reduces numerical difusion troubles and allow a very precise sizing of the finite volumes adjacent to the walls. That can be done by imposing a normal direction adimensional length y^+. This is a great feature when dealing with turbulence models, as the precise calculation of the in boudary layer flow relies on the mesh quality.

Table 2. Geometrical parameters

Parameter	*Nomenclature*	*Value*
Number of main blades	n_b	6
Number of splitter blades	n_s	6
Radial distance at shroud	r_1s	9.372 mm
Radial distance at hub	r_{1h}	2.536 mm
Radial distance of outlet	r_2	18.682 mm
Impeller axial length	L_z	11.37 mm
Leading edge blade angle at shroud	β_{1bs}	50°
Leading edge blade angle at hub	β_{1bh}	17.88°
Trailing edge blade angle	β_2	-50°
Trailing edge width	b_2	1.71 mm
Main blade length	L	25.0 mm
Splitter blade length	L_s	17.5 mm
Blade tip gap	ϵ	0.254 mm
Blade thickness	t	0.762 mm
Wrap angle	ξ	87.5°

The meshes were generated using ANSYS Turbogrid. Three levels of progressive mesh refinements were applied decreasing the adimensional distance y^+ which leads to finer meshes near the walls as showed on Fig. 2.

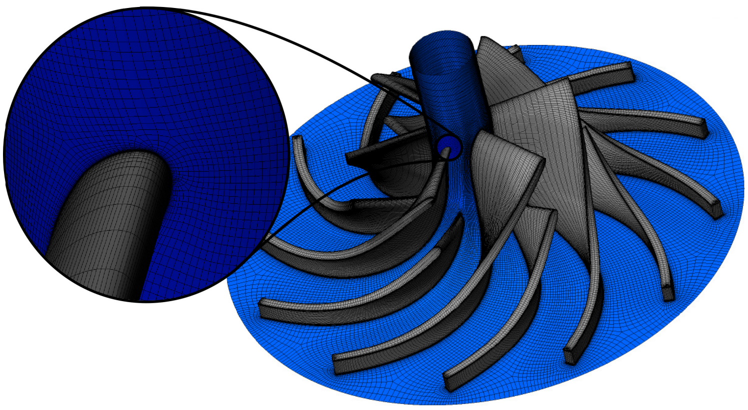

Figure 2. Near-wall mesh refinement.

4.2 Boundary and initial conditions

For computational costs reduction only a single flow path region containing one main and one splitter blade was solved. To mimic the complete set of six flow paths interconnected, two periodic surfaces must be defined, Fig. 3. This assumption may force artifical symmetry on the flow flield, but it is therefore acceptable as the problem was assumed to occur at steady state condition.

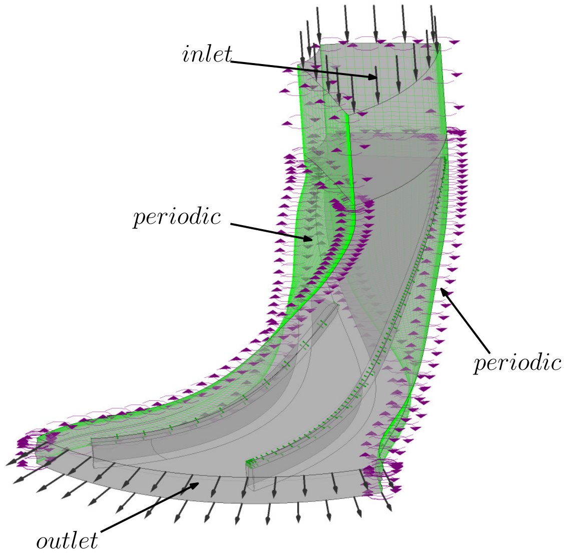

Figure 3. Boundary conditions of flow path.

A common approach to define the boundary conditions of compressible flows is to set up mass flow and total pressure at inlet and a prescribed static pressure at outlet, **(author?)** [Monge]. In fact, if there is no unsteady phenomena a total pressure and temperature at inlet and mass flow at outlet is also a well posed boudary condition, as pointed out by **(author?)** [Benneke] and **(author?)** [Everitt]. The values imposed for the boundary conditions are presented on Table 3. The flow direction at inlet was assumed to be perfect normal to the surfuce, with no pre-swril structures. At the outlet, the mass flux was considered uniform, this assumpution is acceptable as we previously assumed no unsteady phenomena occuring at outlet. All the solid walls are treated as adiabatic and the no-slip condition was employed at them.

Table 3. Total thermodynamic properties at inlet and mass flow conditions.

Property	Value
T_{01}	$305.3\ K$
P_{01}	$7.69\ MPa$
$\dot{m}$	$3.53\ kg/s$

For the initial condition, a turbulence intesity of 1% was prescribed at inlet for all the cases. The coarse mesh is the first one to be computed. ANSYS CFX guessed a preliminary velocity and pressure flow field based on the boundary conditions applied. For subsequent computations, the intermediate and fine meshes were initialized with the converged solution obtained from the previous less refined mesh. This procedure can reduce computational time required for the higher resolution grids and also permits a most stable convergence. For each simulation, the solution was considered converged as soon as the residuals does not decrease anymore, the root mean square residual for the three components of the momentum and the mass equation was obtained at 10^{-4} order.

5 Grid independence study

The computation was carried over a 20 core workstation, powered by two Intel Xeon $E5-2630$ processors provided by $32\ GB$ of RAM. To accomplish a grid convergence index study the number of finite volumes on each grid was ajusted to result on a refinment factor $r \sim 1.3$. Table 5 sumarizes the resulting pressure ratio (PR) and computation times. According to a grid convergence index parameter the intermediate grid was capable to achieve very low numerical error related to domaind discretization.

Table 4. Mesh sizing parameters and total computation time.

Parameter	N° of volumes	blade surface y^+	r	PR	GCI	Total CPU time
Coarse	395928	500	-	1.254	0.12 %	$2h\ 15min\ 48s$
Intermediate	887560	50	1.307	1.253	0.11 %	$3h\ 19min\ 50s$
Fine	1982700	5	1.309	1.262		$15h\ 24min\ 50s$

5.1 Validation

The intermediate grid results was validated against experimental data, very small relative error on pressure ratio predictions and mass flow indicates the numerical results accuratelly predicted real fluid flow behavior, Table 5.

Table 5. Numerical Validation

	CFD	Experimental	Relative error
PR	1.253	1.27	-0.13 %
P_{02}	9.951 MPa	9.96 MPa	-0.09 %
$\dot{m}$	2.04297 kg/s	2.043 kg/s	0.00 %

6 Results

An increment on pressure and temperature along the flow path, as expected for a centrifugal compressor can be seeing at Fig. 4 and Fig. 5. At the leading edge, the reduction of cross sectional area induces an acceleration of the fluid reducing the static pressure and temperature. This undesirable pressure decrease, also known as suplementary depression, can induce a phase change of CO_2, leading to increased internal losses.

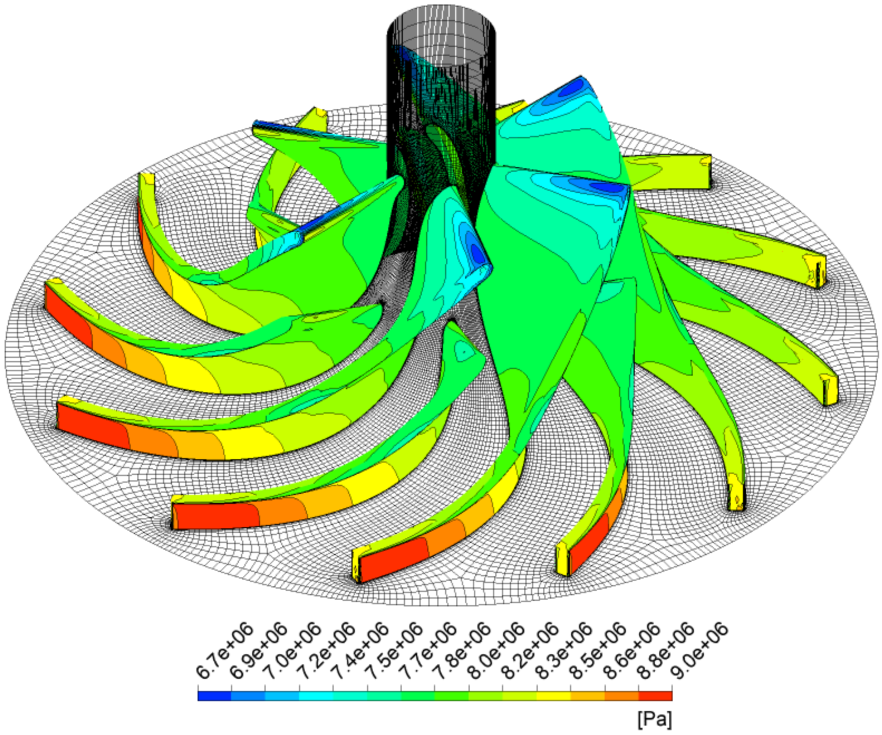

Figure 4. Pressure distribution over blade surfaces.

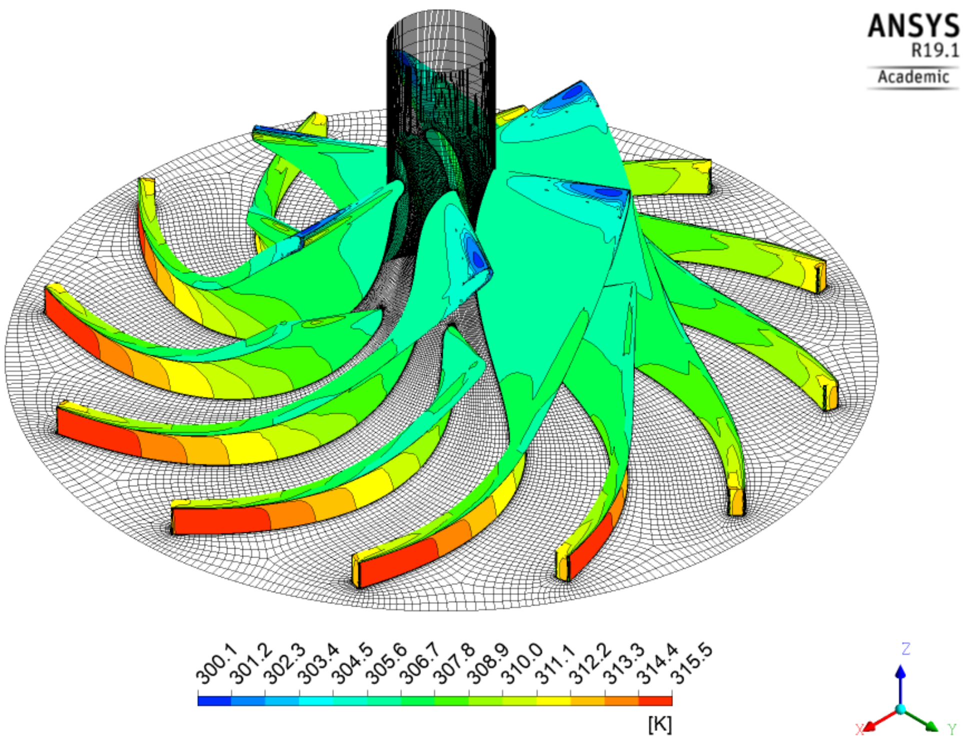

Figure 5. Temperature distribution over blade surfaces.

Figure 6 shows a description of the the thermodynamic states for each point over the blade surface represented on a Temperature-Entropy diagram, despite at the low temperatures and pressures at the leading edge, there was no condensation point. However, at some points CO_2 becomes a gas very close to its saturation condition.

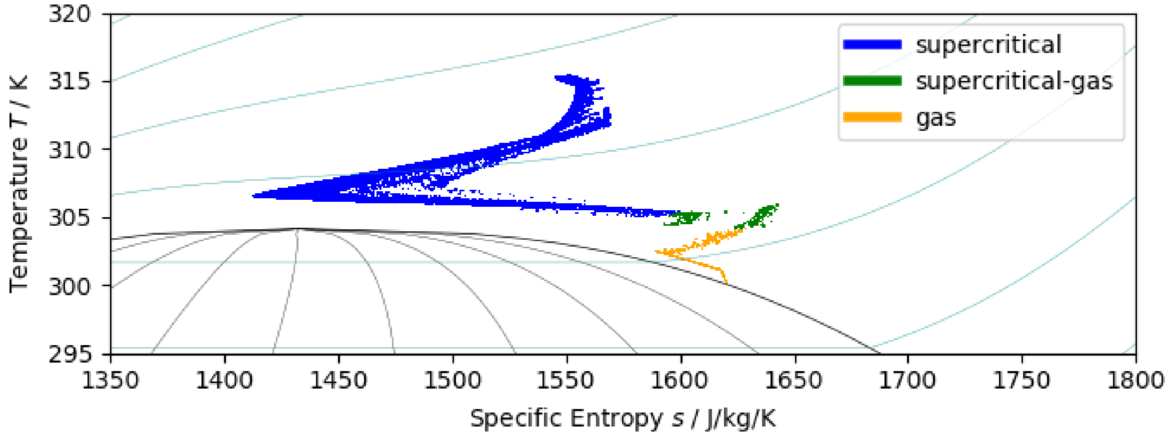

Figure 6. Thermodynamic states over blade surface

Abrupt changes on thermodynamic properties near the blade leading edges was observed. Fig. 7 and 8 shows streamwise distributions of density and velocity along the impeller. Even if the fluid does not chage its phase, as the fluid approaches its critical point the numerical simulation becomes challenging due to the strong variation of thermodynamic properties, as discussed on Section 2.1.

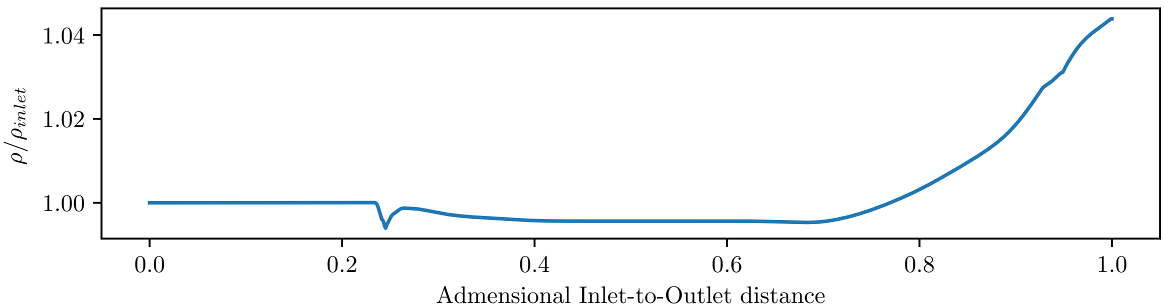

Figure 7. Streamwise variation of density

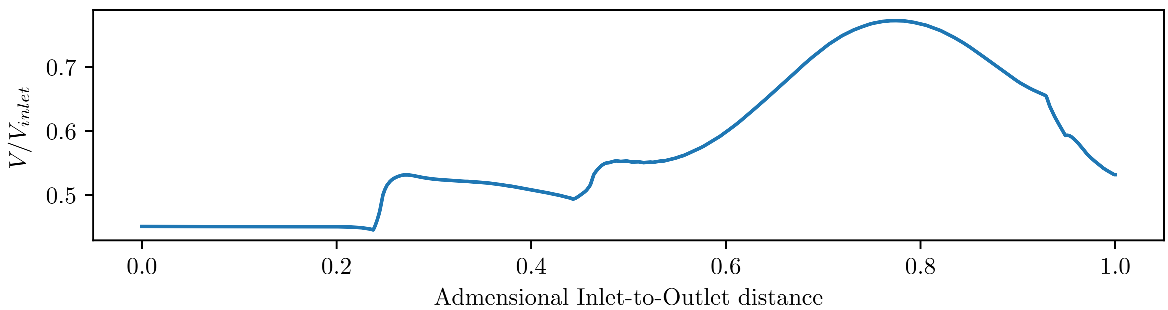

Figure 8. Streamwise variation of velocity

A Mach contour plot can be viewed at Figure 9. It reveals a local acceleration region just after the leading edge stagnation point. This is a critical location for bounadry layer separation. Also from overall

Mach ranges it can be concluded that the impeller operates far from its choking condition, meaning shock losses is not a concern.

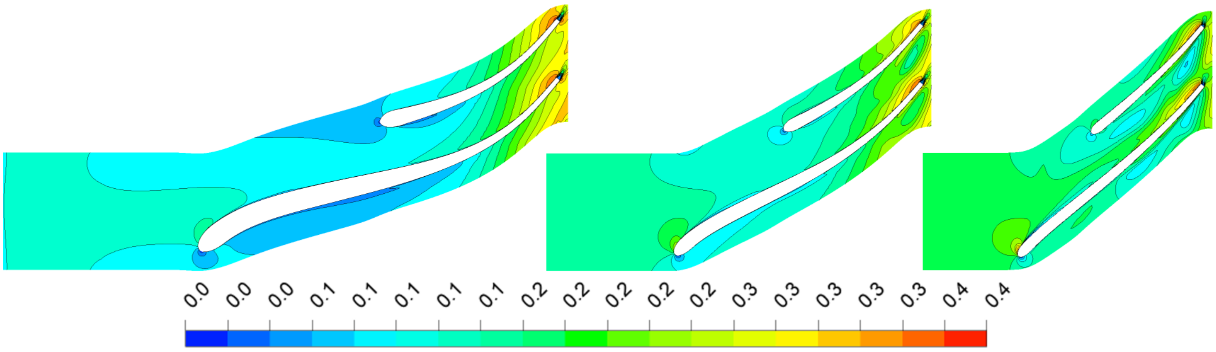

Figure 9. Mach contour plot at blade-to-blade surfaces: 20%, 50% and 80% spanwise location from left to right

The meridional contour plot of pressure distribution on Fig. 10 shows an adverse gradient pressure throughout the flow path. Adjacent to the hub surface, on the region of the clearance gap, the pressure field experiment changes on its gradients, this may induce the boundary layer to detach. That prediction is confirmed by an elucidative 3D plot of the streamlines.

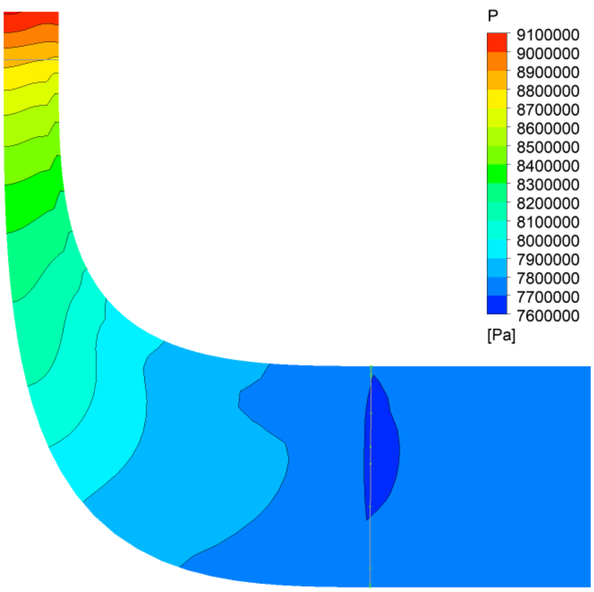

Figure 10. Meridional Plot of Pressure

A very important source of losses that can be predicted by high fidelity computation fluidynamics comprises the losses induced by secondary flows. Fig. 11 shows the streamlines over the flow path, here becomes evident the importance of the splitter blades on the reestabilization of the perturbed flow. As the fluid enters on the impeller the portion travelling on the tip clearance gap experiments pressure gradients that abruptly changes its direction inducing a boundary layer separation over the suction side of the main blade. The vortical structures would propagate along fluid path potentially causing a stall. Splitter blades acts reestabilizing the flow, providing a laminar region over its pressure surface.

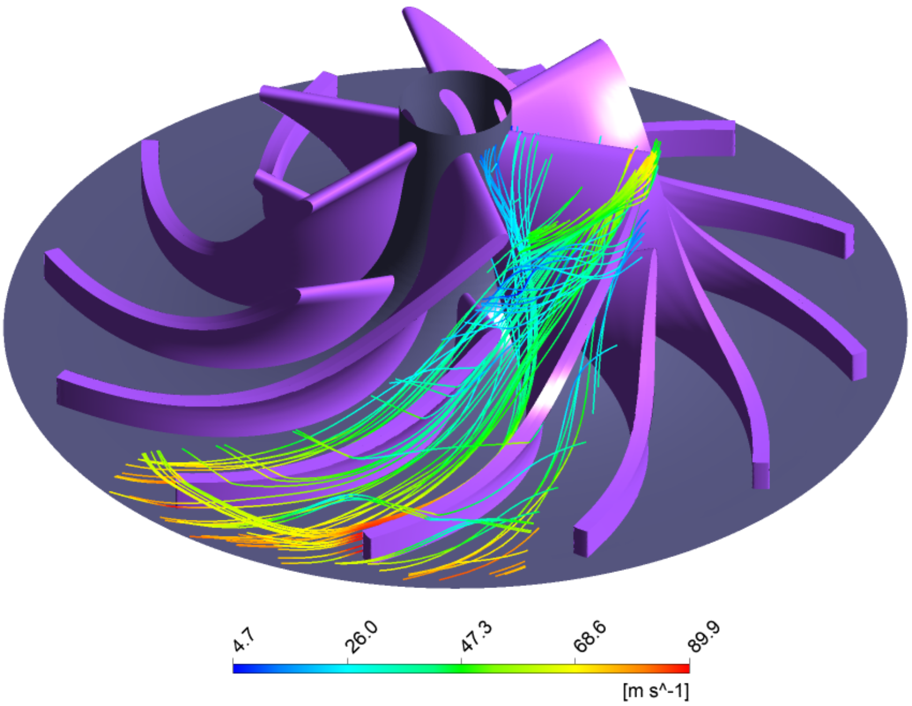

Figure 11. Three-dimensional streamlines.

Figure 12 shows the variations of the pressure and velocity field, with a change on the pressure and velocity gradient direction near the shroud as an effect of the fluid flow trhough the clearance gap.

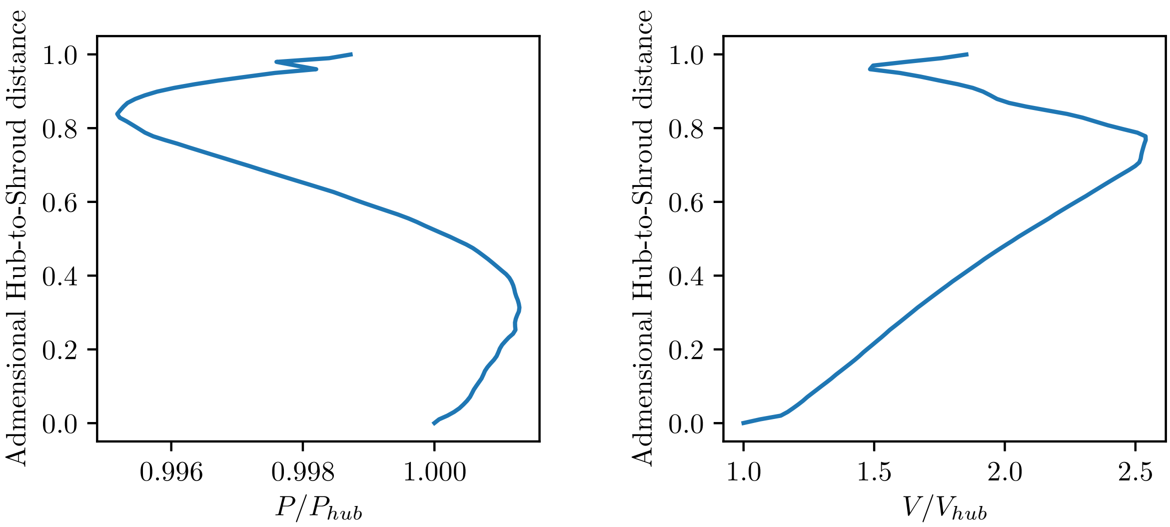

(a) (b)

Figure 12. Spanwise distribution of pressure(12a) and velocity(12b) at 0.5 blade length

7 Conclusion

The numerical simulation of a microcompressor operating with supercritical CO_2 was conducted by solving the RANS equations with a turbulence model $k - \omega\ SST$ using the ANSYS CFX CFD solver. The fluid flow was considered compressible, viscous, turbulent and at steady-state condition. For thermodynamic properties evaluation the Redlich-Kwong equation of state was used. The grid convergence study indicated low numerical errors related to the domain discretization, and the results were on a good agreement with the experimental data. It can be concluded that CFD is a reliable analysis tool for turbomachinery design operating with supercritical CO_2. With main characteristics of internal flow of centrifugal compressors capturated:

- The adverse pressure gradient and positive temperature gradient.
- The presence of acceleration regions just after the stagnation points at blade leading edges with a consequent formation of a suplementary depression zone at the inlet of the impeller.
- The onset of thermodynamic states very close to the saturation line.
- A Secondary flow formation induced by the tip clearance leakage flow and the important function of the splitter blades preventing it to propagate along the flow path.

Acknowledgements

The authors would like to tanks Research Centre for Gas and Innovation for the finnacial support.

References

[Angelino] Angelino, G. Carbon dioxide condensation cycles for power production. vol. 90, n. 3, pp. 287. 1

[Feher] Feher, E. The supercritical thermodynamic power cycle. vol. 8, n. 2, pp. 85–90. 1

[Zhang et al.] Zhang, D., Wang, Y., & Xie, Y. Investigation into off-design performance of a s-CO2 turbine based on concentrated solar power. vol. 11, n. 11, pp. 3014. 1

[Wright et al.] Wright, S. A., Radel, R. F., Vernon, M. E., Pickard, P. S., & Rochau, G. E. Operation and analysis of a supercritical CO2 brayton cycle. Technical report. 1, 3

[Fu and Gundersen] Fu, C. & Gundersen, T. Carbon capture and storage in the power industry: Challenges and opportunities. vol. 16, pp. 1806–1812. 1

[Baltadjiev et al.] Baltadjiev, N. D., Lettieri, C., & Spakovszky, Z. S. An investigation of real gas effects in supercritical CO2centrifugal compressors. vol. 137, n. 9, pp. 091003. 1

[Lettieri et al.] Lettieri, C., Baltadjiev, N., Casey, M., & Spakovszky, Z. Low-flow-coefficient centrifugal compressor design for supercritical CO2. vol. 136, n. 8, pp. 081008. 1

[Pecnik et al.] Pecnik, R., Rinaldi, E., & Colonna, P. Computational fluid dynamics of a radial compressor operating with supercritical CO2. vol. 134, n. 12, pp. 122301. 1, 3.1

[Abramian and Howard] Abramian, M. & Howard, J. H. G. Experimental investigation of the steady and unsteady relative flow in a model centrifugal impeller passage. vol. 116, n. 2, pp. 269. 1

[Lennemann and Howard] Lennemann, E. & Howard, J. H. G. Unsteady flow phenomena in rotating centrifugal impeller passages. vol. 92, n. 1, pp. 65. 1

[Guo et al.] Guo, D., Shi, D., & Zhang, D. Investigation on steady and unsteady performance of a SCO2 centrifugal compressor with splitters. vol. 21, n. suppl. 1, pp. 185–192. 1

[Johnston] Johnston, J. P. Effects of system rotation on turbulence structure: A review relevant to turbomachinery flows. vol. 4, n. 2, pp. 97–112. 1

[Aungier] Aungier, R. H. *Centrifugal Compressors: A Strategy for Aerodynamic Design and Analysis*. ASME Press. 2.1

[Meroni et al.] Meroni, A., Zühlsdorf, B., Elmegaard, B., & Haglind, F. Design of centrifugal compressors for heat pump systems. vol. 232, pp. 139–156. 3.1

[Monge] Monge, B. *Design of supercritical carbon dioxide centrifugal compressors*. PhD thesis. 3.1, 4.2

[Rinaldi et al.] Rinaldi, E., Pecnik, R., & Colonna, P. Computational fluid dynamic simulation of a supercritical CO2compressor performance map. vol. 137, n. 7, pp. 072602. 3.1

[Benneke] Benneke, B. A methodology for centrifugal compressor stability prediction. Master's thesis. 4.2

[Everitt] Everitt, J. N. Investigation of stall inception in centrifugal compressors using isolated diuser simulations. Master's thesis. 4.2